

Hepatobiliary Kinetics of Technetium-99m-IDA Analogs: Quantification by Linear Systems Theory

Shawn Araikum, Trevor Mdaka, Jan D. Esser and Michele Zuckerman

Departments of Nuclear Medicine and Pediatrics, University of the Witwatersrand, Johannesburg, Republic of South Africa

A compartmental model describing the extraction and disposition of ^{99m}Tc -acetanilidoiminodiacetic acid (IDA) compounds by the liver has been applied to 5 adult patients admitted for cholecystitis investigations and 29 jaundiced infants the majority of whom were clinically differentiable into neonatal hepatic and biliary atretic groups. **Methods:** In each case kinetic rate constants were calculated to describe hepatocyte extraction of ^{99m}Tc -IDA structural analogs from blood pool (k_{21}) and subsequent elimination (k_3) of this compound into biliary tract. Also modeled was the reverse-binding constant (k_{12}) describing the return of such radiotracer to the systemic circulation and the blood fraction (f) which accounted for the composite vasculature forming a matrix in the liver. **Results:** It was shown that these indices could be used to determine accurate compartmental mean residence times (MRT^cs) for each patient by correlation with values obtained by deconvolutional analysis and independent measurement of leading edge parenchymal transit times. For the adult patients the following indices, typical of good hepatocyte function, were derived: $k_{21} = 0.933 \pm 0.488 \text{ min}^{-1}$, $k_{12} = 0.0277 \pm 0.0340 \text{ min}^{-1}$, $k_3 = 0.1610 \pm 0.0531 \text{ min}^{-1}$, $f = 0.3519 \pm 0.3048$ and $\text{MRT}^c = 11.19 \pm 3.13 \text{ min}$. Analysis of the pediatric group revealed no significant differences in their respective MRT^cs. However, significant differences in the extraction ($p < 0.01$) and excretion ($p < 0.001$) coefficients were prominent.

Conclusion: This method can be applied to provide accurate and meaningful intercompartmental rate parameters and MRT^cs for adults, nonobstructed and obstructed infants.

Key Words: technetium-99m-IDA; cholecystitis; neonatal cholestasis; compartmental and deconvolutional analysis

J Nucl Med 1996; 37:1323-1330

Qualitative hepatobiliary scintigraphy with ^{99m}Tc -IDA derivatives has been evaluated independently by Gerhold et al. and Majd et al. (1,2) as a diagnostic aid in groups of cholestatic infants. Results of this work demonstrated viability of such modalities in assessing the patency of biliary structures thereby augmenting other methods such as serial ultrasonic examination (3) in arriving at therapeutic decisions.

Limitations of qualitative visual assessment in its application to infants with severe liver dysfunction imposed by observer-dependence when interpreting images led to the development of semiquantitative analytical approaches (4-6). These comprised measurement of 10-min hepatic indices, a 4-min uptake-index and a measurement of the magnitude of radiotracer in duodenal juice aspirates. However, such methodology for determining a 10-min hepatic index was re-evaluated and found to be unreliable in assessing the benefits of surgery. Alternately the 4-min uptake-index has not gained widespread acceptance because it disregarded important plasma exit routes and contributions from an extravascular component in its analysis resulting in an overestimation of hepatic extraction of radiotracer. Despite the success of radiotracer content determinations in duodenal juice aspirates, this modality has also not gained general acceptance

for the investigation of cholestatic neonates—probably because the insertion of a fluoroscopy-guided nasogastric tube into the duodenum is considered invasive.

Further development in semiquantitative analysis of hepatobiliary function entailed: (a) theoretical formulation of pharmacokinetic models to determine disposition indices of IDA-analogs (5,7,8) from measured disappearance of radiotracer from peripheral blood and (b) deconvolutional analysis of liver time-activity curves (TACs) when the blood curve is applied as input function (9-14). A cited disadvantage (15,16) of the latter technique is that it did not account for the vasculature of the liver, any region of interest of which contains blood vessels and an extravascular component. An analysis by such techniques therefore describes the composite response of hepatocyte, intrahepatic bile duct and the latter-mentioned structures describing vasculature. In order to interrogate hepatocyte activity and patency of the biliary system, compartmental analysis based on the approach of Hawkins et al. (17-19) was developed for quantitative evaluation of our group of cholestatic infants.

The methodological approach of this paper is to develop and apply four basic compartmental configurations to describe blood and liver TACs in a group of five adult patients investigated for chronic cholecystitis who otherwise demonstrated good handling of IDA. The best configuration describing this group of subjects was then used as a template for the infants to extract maximal information for intercompartmental rate processes and hence compartmental mean residence times. Incorporated in this method for the validation of such parameters is: (a) the measurement of leading edge parenchymal transit times and (b) calculation of MRTs by deconvolutional analysis. Further usefulness of such measurements in interpreting the results of the pediatric studies followed in natural progression and are given in the latter part of the paper.

MATERIALS AND METHODS

Patients and Data Acquisition

A group of five adult subjects (mean age, 73 ± 7 yr) admitted with right, upper-abdominal pain and investigated routinely for chronic cholecystitis was used in preliminary model evaluation. Exclusive use was made of subjects showing good extraction and clearance of ^{99m}Tc -diisopropyl-IDA (^{99m}Tc -DISIDA) on qualitative scintigraphic analysis. In each case an impulse bolus of 185 MBq activity was injected intravenously on commencement of the respective study. Pre-treatment comprised overnight fasting to facilitate prompt gallbladder filling.

For the pediatric patients (mean age, 6 ± 3 wk) pre-treatment comprised an oral administration of $5 \text{ mg kg}^{-1} \text{ day}^{-1}$ phenobarbital for three days prior to scintigraphic assessment. Such scintigraphy was initiated with the intravenous injection of a 37-MBq impulse bolus of ^{99m}Tc -trimethylbromo-IDA (^{99m}Tc -mebrofenin). Patients were clinically diagnosed and grouped as follows: 14 neonatal hepatitis, 13 biliary atresia, 1 Alagille's Syndrome and 1

Received Feb. 15, 1995; revision accepted Oct. 20, 1995.

For correspondence or reprints contact: Shawn Araikum, Cavendish Laboratory, Cambridge University, Cambridge CB3 0HE, United Kingdom.

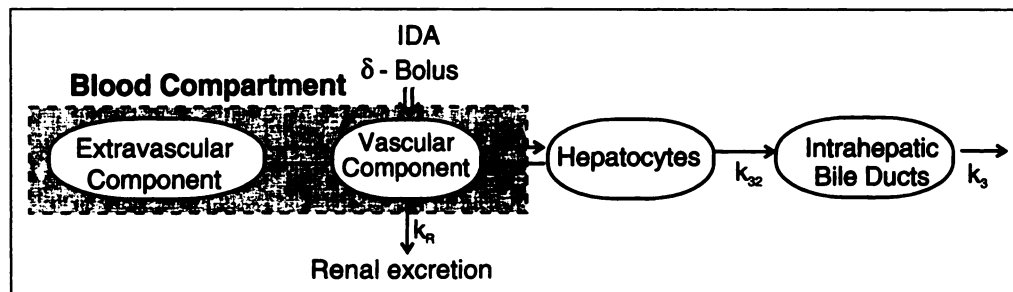


FIGURE 1. Multicompartmental configuration for IDA-analog compound distribution in blood and liver.

choledochal cyst. In the latter instance, scintigraphy was performed before and after surgery.

In all studies data were acquired in the anterior projection over the abdomen and thorax for 1 hr. A large field of view gamma camera with low-energy, medium-resolution collimators interfaced to a computer and display system was used for data acquisition. Frames were taken in dynamic word-mode at 30-sec intervals with a spatial matrix resolution of 64×64 pixels square.

Data Analysis and Model Selection

Time-activity curves (histograms) were generated on a processor for subsequent analysis and manipulation. This was achieved by drawing circular regions of interest (ROIs) of equal area for each subject over the heart-left ventricle and upper right lobe of the liver. Care was taken to exclude major biliary ducts from the liver ROI. Histograms generated in this way described the total counts detected per unit time in each region as a function of time. These data were then transferred to floppy disk, in ASCII format, for analysis. Regression subroutines were written in FORTRAN for use with the MINUIT multivariate regression software (CERN, Geneva). All data were corrected for radioactive decay in this procedure. Optimum solutions were derived by this algorithm when the sum square of individual data point errors (SSQ) was minimized. Another implied constraint was that such searches for solutions converge when the estimated distance to minimum SSQ was less than $0.1 \text{ counts}^2 \text{ sec}^{-2}$ and the fractional change in the covariance matrix was less than 0.04.

Preliminary model analysis comprised parameter estimation from a given data set when the data was grouped in 30-, 60- and 90-sec intervals. This was done to assess the stability of the technique and loss in accuracy which might result from prolonged frame acquisition times. The dependence of parameter estimation on the total study time was derived by performing regressions when the data was not truncated and when it was truncated at 20, 30 and 40 min.

Essential to the analysis of patient data was the evaluation of various model configurations. Combinations of five basic configurations were analyzed. These were cases in which:

1. The measured heart-left ventricular blood curve was used as input function to the liver.
2. The blood curve was modeled theoretically by using a Gaussian distribution of given height (activity), dispersion and temporal location (all determined a priori from the measured blood curve) to describe the input function for the blood compartment.
3. It was assumed that the hepatocyte forward disposition rate was identical to the intrahepatic bile duct disposition rate.
4. The uniqueness of the disposition rates discussed in (3) was prescribed.
5. It was assumed that the reverse-binding rate constant $k_{12} > 0$ and $k_{12} = 0$, respectively.

Figure 1 depicts a schematic representation of the multicompartmental model which forms the basis for this analysis. Two criteria used for model selection, as recommended by Landaw and DiSte-

fano (20) for optimal parameter identifiability viz. the Akaike information criterion (AIC) and the Schwarz criterion (SC), are given in Equations 1 (a) and (b). These are a function of the number of data points (N_{data}), the number of model parameters (N_{par}) and the minimized SSQ derived in each optimization procedure.

$$\text{AIC} = N_{\text{data}} \cdot \ln(\text{SSQ}) + 2 \cdot N_{\text{par}} \quad \text{Eq. 1a}$$

$$\text{SC} = N_{\text{data}} \cdot \ln(\text{SSQ}) + N_{\text{par}} \cdot \ln(N_{\text{data}}) \quad \text{Eq. 1b}$$

In both cases, the second term acts as penalty function for models with more parameters. The model with the lowest combined information criteria was taken to be the most favorable descriptor for the data. Complementary to this analysis was the computation of associated correlation matrices for each regression procedure which could be inspected to provide assessments of error propagation from the kinetic indices thus determined.

Significance Testing

Statistical analysis was performed for the assessment of the degree to which significant difference in the patient groupings could be identified. This was achieved by performing the unpaired Student's t-test. Patient groupings were taken to typify distinct behavior for p-values < 0.05 .

THEORETICAL METHODS

General Framework

The starting point of this analysis entailed an assumption of linear tracer kinetics to describe extraction and elimination of the group of IDA-analog compounds by hepatocytes. This assumption, rather than the prerequisite of Michaelis-Menten kinetics, is generally taken to be true (19) when tracer quantities are used. The implication is that there is no appreciable saturation of receptors for radiotracer. Given such a premise linear system theory has been applied to derive kinetic indices (k_{ij}) from liver and blood time-activity curves for use in good health and disease.

Generally, the problem to be solved by linear system theory can be posed as follows:

$$\frac{dx^j(t)}{dt} = A_{ji}x^i(t) + B_{ji}u^i(t) \quad \text{Eq. 2}$$

$$x^j(t) = e^{A_{ji}t}x^i(0) + \int_0^t d\tau e^{A_{ji}(t-\tau)}B_{ji}u^i(\tau) \quad \text{Eq. 3}$$

In matrix Equation 2 the Einstein summation convention applies and in the standard nomenclature the $x^i(t)$, $j, i = 1 \dots n$ with $n =$ number of compartments, describe the time (t) evolution of radioactivity in each compartment, A_{ji} describes the flow into and out of each compartment by the first order kinetic, $u^i(t)$ are the input control functions for each compartment and B_{ji} is the matrix describing the method of control application. Solutions to this problem can be obtained (21) when the transition matrix $\exp(A_{ji}t)$ is determined and are given by Equation 3, with $x^i(0) = 0$ for all $i = 1 \dots n$ as initial conditions.

Model for the Liver Curve

For this analysis the blood compartment was not modeled explicitly. Rather, the measured blood time-activity curve ($B_c(t)$) derived from a heart-left ventricular ROI was used to describe the input to the liver. The magnitude of this component was taken to be $k_{21} * B_c(t)$ and incorporated into Equation 3. In this case solutions for the rate parameters were derived from:

$$y(t) = x^1 + x^2 = k_{21} \int_0^t \{a_{11}(t - \tau) + a_{21}(t - \tau)\} B_c(\tau) d\tau$$

$$a_{11}(t) = e^{-(k_{32}+k_{12})t}, a_{21}(t) = \frac{k_{32}}{k_{32} + k_{12} - k_3} \{e^{-k_3 t} - e^{-(k_{32}+k_{12})t}\}$$

Eq. 4

In each case, the theoretically modeled activity over the liver region of interest ($L(t)$) was therefore specified by:

$$L(t) = y(t) + f * B_c(t) \quad \text{Eq. 5}$$

f being the fraction of the measured blood curve superimposed on hepatocyte and intrahepatic bile duct activity. This final expression was used in a nonlinear regression of the liver time-activity curve ($L_c(t)$) for parameter estimation.

$$MRT^c = \frac{\int_0^\infty d\tau y(\tau)}{y(0)} \quad \text{Eq. 6}$$

In this way effects of extrahepatic activity on the estimation of mean residence times for the liver were obviated as $y(t)$ provides the contribution to the liver curve from hepatocytes and intrahepatic bile ducts, excluding liver vasculature.

To theoretically determine mean residence times from Equation 6 the above calculation was repeated for the situation in which a unit bolus, represented by the Dirac-delta function ($\delta(t)$), was applied instantaneously at time $t = 0$ min. This yielded the following for $y(t)$ in terms of the k_{ij} :

$$y(t) = k_{21} \left(1 - \frac{k_{32}}{k_{32} + k_{12} - k_3} \right) e^{-(k_{32}+k_{12})t} + \frac{k_{32}k_{21}}{k_{32} + k_{12} - k_3} e^{-k_3 t}$$

Eq. 7

from which the following expressions for the MRT^c can be shown to apply:

$$MRT^c = \left(1 - \frac{k_{32}}{k_{32} + k_{12} - k_3} \right) \left(\frac{1}{k_{32} + k_{12}} \right) + \frac{k_{32}}{k_3(k_{32} + k_{12} - k_3)}$$

Eq. 8

when $k_{12} = 0$:

$$MRT^c = \frac{1}{k_{32}} + \frac{1}{k_3} \quad \text{Eq. 9a}$$

and k_{32} equals k_3 :

$$MRT^c = \frac{2}{k_{12} + k_3} \quad \text{Eq. 9b}$$

When intrahepatic bile ducts are obliterated (in biliary atretic patients, for example) or nonfunctional (neonatal hepatic subjects with acute edema), it is useful to consider, individually, hepatocyte and intrahepatic bile duct MRT^c for comparative purposes in health and disease. For the hepatocyte compartment:

$$MRT^c = \frac{1}{k_{32} + k_{12}} \quad \text{Eq. 10a}$$

and the intrahepatic bile duct compartment:

$$MRT^c = \frac{k_{32}}{k_{32} + k_{12} - k_3} \left(\frac{1}{k_3} - \frac{1}{k_{32} + k_{12}} \right) \quad \text{Eq. 10b}$$

Model for the Blood Curve

Similar analysis, as applied for the liver data, was undertaken for the description of the blood washout curve. This yielded the following expression for the activity of radiotracer in the blood compartment:

$$B(t) = \int_0^t d\tau e^{-(k_{21}+k_R)(t-\tau)} \{G(\tau) + k_{12}L_c(\tau)\}$$

$$G(t) = h_0 * e^{-(t-t_0)^2/\Gamma} \quad \text{Eq. 11}$$

No overt analysis was undertaken to describe all extravascular components or recirculations in the blood pool. However, the renal route of excretion was modeled explicitly to enable adequate description of obstructed infants who show urinary bladder activity. The input to the blood compartment for this model was described by $G(t) + k_{12} * L_c(t)$ with the leading term describing the method of bolus introduction and the second term accounting for reverse-binding from the liver. In describing the method of bolus introduction, which was applied as a rapid impulse, the Gaussian function ($G(t)$) was chosen primarily because it forms a legitimate element of convergent delta sequences (22).

For the determination of blood MRT^c , expression 6 was also applicable for the situation in which a unit bolus was used as input to the blood compartment, i.e. when:

$$B(t) = \int_0^t d\tau e^{-(k_{21}+k_R)(t-\tau)} \delta(\tau) \quad \text{Eq. 12}$$

yielding:

$$MRT^c = \frac{1}{k_{21} + k_R} \quad \text{Eq. 13}$$

In this analysis the question of parameter identifiability for k_{21} and k_R requires special consideration as these variables only ever appear together as a sum throughout this analysis. Any independent regression of the measured blood curve can only be expected to give a reliable measure of $k_{21} + k_R$, as opposed to an estimate of k_{21} and k_R individually. While such an estimate of the sum of these indices might be reliable for MRT^c determination (Eq. 13) it does not provide maximal information for liver and renal extraction uniquely. To circumvent this problem, and determine the liver extraction rate constant (k_{21}) from measured blood curve in doing so, the renal extraction rate k_R was derived from the cumulated urinary bladder activity as follows:

$$k_R = \frac{UB(60 \text{ min})}{\int_0^{60 \text{ min}} d\tau B_c(\tau)} \quad \text{Eq. 14}$$

where $UB(60 \text{ min})$ is the cumulated urinary bladder activity 60 min post-IDA administration and $B_c(t)$ is the measured blood time-activity curve defined earlier. In instances where patients voided before the end of the study, the 60-min limit imposed was substituted with the time preceding this event. All urinary bladder measurements were corrected for background counts from activity in interstitial tissue. This value was derived from the 2-min urinary bladder ROI activity measurement.

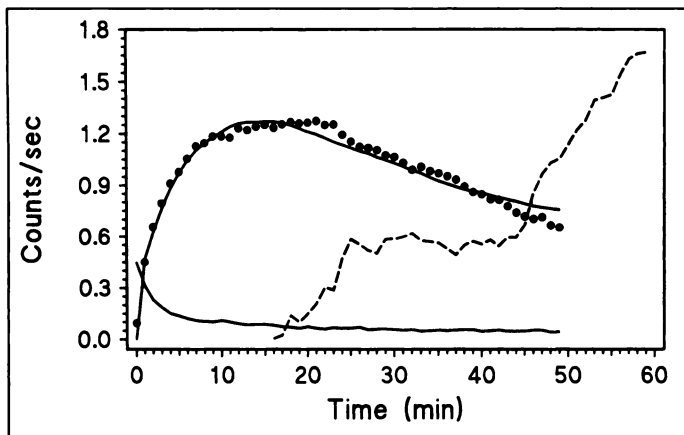


FIGURE 2. Optimized theoretical liver curve (solid line) and data (\cdot), the measured blood washout (solid line) and gallbladder (---) curves for Patient 1.

Deconvolutional Analysis

For the purposes of comparison and independent corroboration of the MRT^c calculated by compartmental analysis, the method of Laplace was applied to derive liver mean residence times (MRT^{lap}) from identical data. For this part of the study, blood and liver TACs were described by bi-exponential functions:

$$B(t) = a_1 e^{-\alpha_1 t} + b_1 e^{-\beta_1 t}; L(t) = a_2 e^{-\alpha_2 t} + b_2 e^{-\beta_2 t}. \quad \text{Eq. 15}$$

Using these theoretical forms, it was possible to deconvolute analytically the liver response ($R(t)$) to obtain the expression of Equation 16.

$$R(t) = \frac{1}{a_1 + b_1} \left(\frac{\partial L(t)}{\partial t} + D * L(t) + G \int_0^t d\tau e^{-C\tau} L(t - \tau) \right) \\ \equiv a_3 e^{-\alpha_3 t} + b_3 e^{-\beta_3 t} \quad \text{Eq. 16}$$

here:

$$C \equiv \frac{\alpha_1 b_1 + \beta_1 a_1}{a_1 + b_1}; D \equiv \alpha_1 + \beta_1 - C \quad \text{and} \quad G \equiv \alpha_1 \beta_1 - DC.$$

Mean residence times could thus be determined from a bi-exponential fit of $R(t)$, the expression for which is given below:

$$MRT^{lap} = \frac{\frac{a_3}{\alpha_3} + \frac{b_3}{\beta_3}}{a_3 + b_3}. \quad \text{Eq. 17}$$

Leading Edge Parenchymal Transit Times

Leading edge parenchymal transit times (LEPTTs) were determined from the times of first hepatic duct visualization and radiotracer, gallbladder times of arrival whenever possible. The latter measurement, being demonstrated in detail for Patient 1 data, was performed as follows: To determine the activity of radiotracer in the gallbladder a circular ROI was constructed over this structure and positioned for maximal overlap with liver tissue posteriorly. In all such cases such ROIs were positioned superiorly as close to the gallbladder entrance as possible. A subtraction of the activity in this ROI from that in the liver-right upper lobal ROI therefore gave the magnitude of activity due to radiotracer in the gallbladder exclusively. The result of this analysis is depicted graphically in Figure 2 which contains blood, liver and gallbladder time-activity curves. It is clear from this measurement that the LEPTT is approximately 16.5 ± 0.5 min. This value compares favorably with the calculated MRT^c of 16.13 min thus verifying the patency of the biliary system.

Because leading edge parenchymal transit times measured in this way include biliary duct transit times it can be expected that such values should be larger than calculated compartmental mean residence times. However, error was introduced into the LEPTT measurement by the fact that the volume of liver tissue superimposed on the gallbladder ROI was not necessarily identical to that in the liver-right upper lobal ROI. For this part of the analysis an indication of such uniformity or deviance was assessed from the initial rise of the liver and gallbladder ($GB(t)$) histograms. When these histograms have identical initial rises, in the 0–6 min period typically, a straightforward subtraction technique has optimal accuracy. However, in all cases an attempt to correct for non-uniformity was made by using the following correction factor (CF) for the most general situation:

$$CF = 1 + \frac{\int_0^t d\tau \Omega(\tau) \{L_c(\tau) - GB(\tau)\} / L_c(\tau)}{\int_0^t d\tau \Omega(\tau)}. \quad \text{Eq. 18}$$

This factor incorporates a time-weighted average of fractional gallbladder histogram deviation from liver histogram. Here, $\Omega(t)$ is the nonzero weighting function for the data over the specified domain. Two situations were evaluated in which all data were weighted equally and weighting followed the form, $L_c^{-1/2}(t)$. The latter function is taken to be the approximate inverse standard deviation (s.d.) of such measurements. In these studies the maximum error due to volume nonuniformity was estimated to be as large as 2.0 min.

The significance of such measurements is that calculated mean residence times ought in principle always to be smaller than or equal to measured LEPTTs which can thus be used as a probable least upper bound for MRT^c s.

ADULT STUDIES

Best Model Configuration

An analysis of the information criteria revealed that the best model describing the liver curve was the case in which k_3 and k_{32} were identical with no evidence for a distinct intrahepatic bile duct compartment. Such results are in keeping with previously published data (19). Further analysis has also demonstrated that in subjects with good extraction and excretion (Patients 1 through 3) the model with $k_{12} = 0$ is preferred. In such cases where the SSQ was nearly identical both statistical criteria demonstrated a bias for the model with fewer parameters. However, for the purposes of such studies where aberrant hepatocellular behavior is only suspected and not confirmed the use of the model with $k_{12} > 0$ is advocated. Absolute values for patient kinetic parameters thus determined appear in Table 1. Graphical results of this procedure for Patient 1 data are provided in Figure 2. The points shown are derived from data grouped in 60-sec intervals which is the coarsest resolution used for parameter estimation. The effect of this can be seen in the lack of bolus resolution in the blood curve which begins at a maximum and decreases monotonically.

Further analysis showed that when the global sum square of the errors (SSQ_c) from the blood curve and the liver curve was minimized, differences between these hepatic indices and those derived from the model for the liver curve ($SSQ(L - C)$) were less than five percent. Explicitly, this involved minimizing:

$$SSQ_c = SSQ(B - C) + SSQ(L - C) \quad \text{Eq. 19}$$

TABLE 1
Intercompartmental Rate Parameters and Mean Residence Times for the Adult Subjects

Patient no.	k_{21} (min ⁻¹)	k_{12} (min ⁻¹)	k_3 (min ⁻¹)	f (-)	MRT ^c (min)	MRT ^{exp} (min)
1	0.929	0.0191*	0.1049	0.2700	16.13	10.73
2	1.748	0.0008*	0.2203	0.1991	9.05	6.57
3	0.730	0.0010*	0.2148	0.1204	9.27	6.20
4	0.806	0.0342	0.1256	0.2854	12.52	17.55
5	0.453	0.0832	0.1392	0.8844	8.99	8.49
Mean ± s.d.	0.933 ± 0.488	0.0277 ± 0.0340	0.1610 ± 0.0531	0.3519 ± 0.3048	11.19 ± 3.13	9.91 ± 4.64

*Patients in which the model $k_{12} = 0$ is preferred in terms of the AIC and SC.

where $SSQ(B - C)$ is the SSQ derived from the measured blood curve. For the purposes of illustration, the results of this procedure are given for Patient 1 data: Values consistent with those in Table 1 were obtained for the hepatic curve and the following associated kinetic indices were derived to describe the measured blood activity: $h_0 = 6.146$ counts sec⁻¹ min⁻¹, $t_0 = 0.0241$ min, $\Gamma = 0.0108$ min² and $k_R = 0.3870 \times 10^{-4}$ min⁻¹, respectively.

Alternately, exclusive analysis of the blood curve could not yield consistent values for hepatocyte extraction (k_{21}). The reason postulated for this is that recirculation and exchange from extravascular components plays a significant role in explaining the observed blood time-activity curve. In all blood curve data analyses, the hepatocyte extraction was underestimated to compensate for these effects. As the rectification of such effects necessitates the introduction of further parameters to describe the acquired data, the model using the measured blood curve as input to the liver (described earlier) was preferred. This method intrinsically accounted for any recirculations and exchanges occurring in the blood compartment.

Kinetic Indices and Mean Residence Times

An inspection of the results recorded in Table 1 reveals a mean MRT^c (\pm s.d.) of 11.19 ± 3.13 min for this group which is in good agreement with the values determined by deconvolutional analysis. This value is also in the range of reported LEPTTs (23) in similar groups of patients—these fell in the range of 5–30 min typically. Hallmarks of this patient group comprise the following: (a) relatively high DISIDA extraction rates, $k_{21} > 0.5$ min⁻¹, (b) low relative reverse-binding of radiotracer from liver into blood pool, i.e. average $k_{21}/k_{12} = 599 \pm 938$ and (c) good clearance of DISIDA, viz. $k_3 > 0.1$ min⁻¹ typically. Liver function tests taken routinely for this adult group of patients who were investigated for chronic cholecystitis are given in Table 2.

Such findings are all in keeping with what is expected qualitatively viz. extraction and accumulation of DISIDA in the

liver and subsequent excretion. The accumulation phase in all these subjects is also consistent with their relative values of extraction and elimination viz. $k_3 < k_{21}$ in all cases.

Measurements of urinary bladder activity for the determination of k_R yielded values $< 10^{-5}$ min⁻¹ confirming low renal excretion properties for DISIDA in normal subjects.

PEDIATRIC STUDIES

Kinetic Indices and Mean Residence Times

Graphical results of this analysis are given in Figures 3A and 4A for representative neonatal hepatic and biliary atretic infants. Corresponding scintigraphy of the hepatic patient (Fig. 3B, C, D, E) demonstrated reasonable radiotracer uptake and retention with discernible bowel activity on the later images (Fig. 3E). Figures 4B, C, D, E are typical of the biliary atretic patients viz. poor overall extraction, retention and excretion of radiotracer was evident. This was further confirmed by prominent urinary bladder activity in later scintigraphic images (Fig. 4E).

Furthermore, in the hepatic subject (Fig. 3A) the maximum in the liver curve exceeded that of the blood curve; a clear temporal displacement of these maxima was also evident. Such qualitative observations are consistent with the interpretation of reasonable hepatocyte clearance. In the atretic infant (Fig. 4A), for example, the opposite was true viz. the blood maximum was greater than that of the liver and there was no visual temporal differentiation between these maxima. In both cases such observations were consistent with qualitative scintigraphic impressions and the corresponding numerical results cited.

Numerical results of these studies (Tables 3 and 4) revealed significant differences between the pediatrics with hepatitis and biliary atresia in their extraction (k_{21} ; $p < 0.01$) and excretion (k_3 ; $p < 0.001$) indices. Problematic, however, are the neonatal hepatic patients who behave scintigraphically as do the biliary atretic patients—typical of this sub-group are Patients 7 through 11. Their indices are: $k_{21} = 0.1840 \pm 0.1014$, $k_{12} = 0.0633 \pm 0.0087$ and $k_3 = 0.0025 \pm 0.0050$ min⁻¹, which are not significantly different from the biliary atretic group. This result is similar to those previously published (14) which emphasizes the fact that such subjects in the same clinical group can present in a range of severity. This can be seen by the fact that some neonatal hepatic subjects (Patients 14 and 17, for example) show excellent extraction, others demonstrate intermediate values (Patients 16 and 19), while the greater majority show significantly suppressed extraction.

No significant difference could be found in the mean residence times across the clinical groupings given. Important to note from a modeling perspective is that the situation in which a functional intrahepatic bile duct compartment is postulated provides a mean residence time twice as large as the situation

TABLE 2
Liver Function Test Results for the Adult Subjects

Liver function tests*	Chronic cholecystitis
Total protein (g · L ⁻¹)	73 ± 8
Albumin (g · L ⁻¹)	42 ± 9
Total bilirubin (μmole · L ⁻¹)	16 ± 8
Direct bilirubin (μmole · L ⁻¹)	6 ± 3
Alkaline phosphatase (IU · L ⁻¹)	263 ± 337
Aspartate aminotransferase (IU · L ⁻¹)	18 ± 9
Alanine aminotransferase (IU · L ⁻¹)	21 ± 9

*Values provided as mean ± s.d.

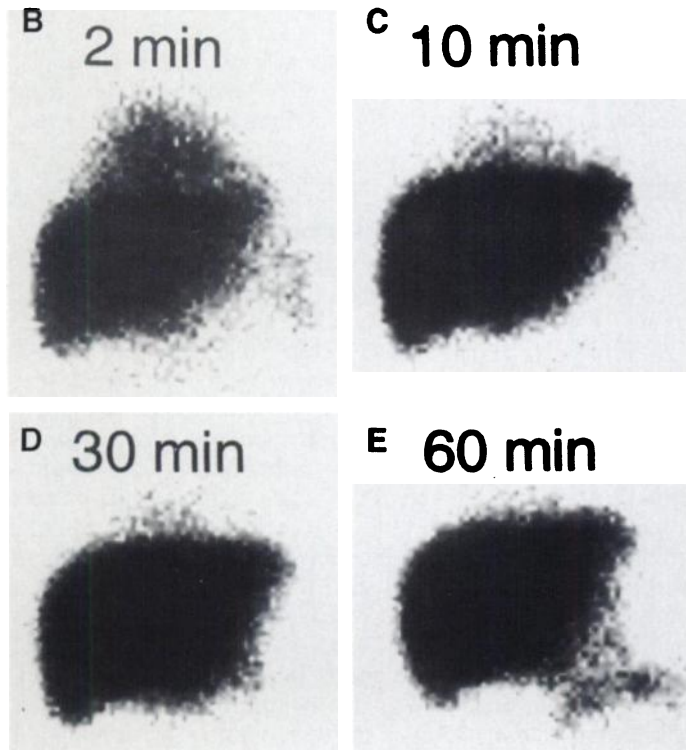
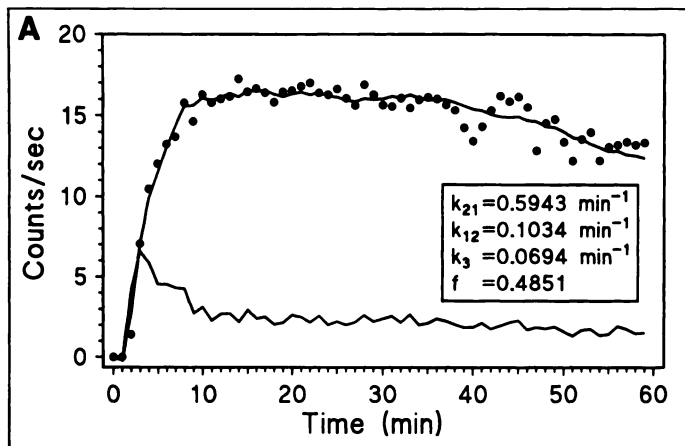


FIGURE 3. (A) Regression liver time-activity curve for an infant presenting with neonatal hepatitis. (B, C, D, E) Scintigraphic images performed at 2, 10, 30 and 60 min, respectively.

where no such compartment is stipulated (Equations 9b and 10a). An inspection of the information criteria and the results obtained from deconvolutional analysis demonstrate a bias for the latter postulate in the majority of biliary atretic patients.

Hepatocyte Extraction Performance Index

In comparing the pediatric subgroups the concept of mean ratio of hepatocyte extraction and reverse-binding rate constants viz. (k_{21}/k_{12}) was introduced. This composite index takes on special significance when it is considered that in the diseased state hepatocyte extraction has been found to be poor and reverse-binding accentuated (19,24). A small value for this ratio is therefore expected in cases of poor function with elevated values signaling better function and prognosis for improved health. This ratio derived for the group classified neonatal hepatitis was 10.68 ± 10.51 in contrast to the biliary atretic group whose mean value was 2.79 ± 1.61 ($p < 0.01$). Both these values are considerably less than the corresponding value derivable from the adult patients who, on the whole, are representative of good hepatocyte function. Because this ratio is

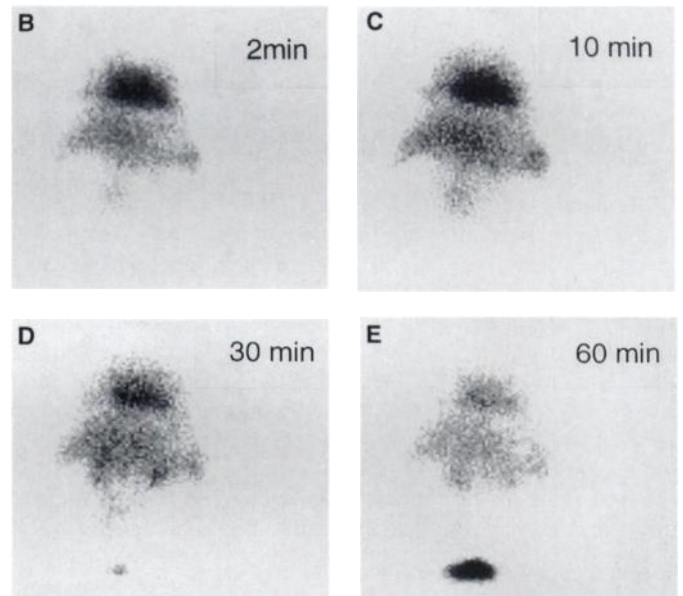
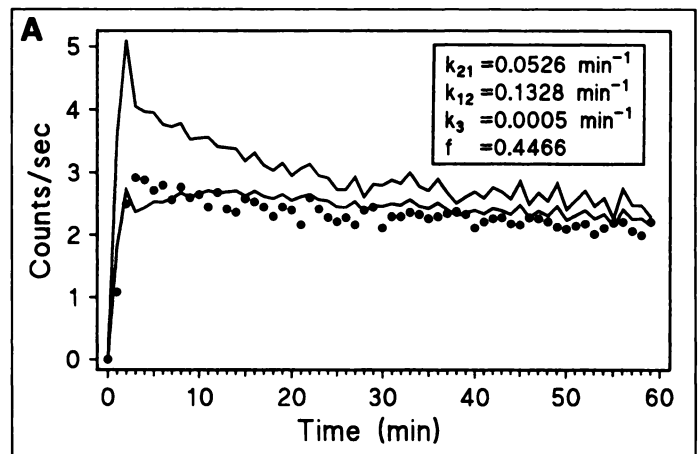


FIGURE 4. (A) Regression liver time-activity curve for an infant with biliary atresia. (B, C, D, E) Hepatobiliary scintigraphy at 2, 10, 30 and 60 min, respectively.

an asymptotic form when $k_{12} \rightarrow 0$, i.e. the case closest to normal function, it is expected that differences due to poor function (in serial studies, for example) would be marked.

Leading Edge Parenchymal Transit Times

The relationship between the MRT^c and LEPTT in the infants demonstrating biliary drainage scintigraphically is given in Figure 5. In all these subjects except one (data point \blacktriangle), the LEPTT values were significantly larger in magnitude which is indicative of prolonged biliary duct transit times. This result can be expected as such subjects often demonstrate obstruction due to edema and partial occlusion of the left and right hepatic ducts. It is also worthy of note that the subject with near identical MRT^c and LEPTT also has a very good extraction rate constant, $k_{21} = 1.1745 \text{ min}^{-1}$, as compared to the other infants.

CONCLUSION

Reliable and accurate intercompartmental rate parameters and MRT^c s can be derived for adult and pediatric subjects via this analysis. Such MRT^c values were compared with independent measure of leading edge parenchymal transit times and found to be consistent. Good correlation was also found between the values of mean residence times determined compartmentally and those derived by deconvolutional analysis.

An advantage of the compartmental analysis performed in

TABLE 3
Kinetic Indices and Derived Mean Residence Times for Pediatric Group

Patient no.	k_{21} (min ⁻¹)	k_{12} (min ⁻¹)	k_3 (min ⁻¹)	k_R^* (min ⁻¹)	f (-)	MRT ^{exp} (min)	MRT ^c (min)
Neonatal hepatitis							
6	0.1752	0.0549	0.0273 [†]	0.68	0.3385	46.20	24.33
7	0.3261	0.0740	0.0000	0.54	0.7134	12.61	13.52
8	0.0754	0.0515	0.0113	3.07	0.5866	20.30	15.92
9	0.0999	0.0693	0.0000	3.50	0.5510	21.15	14.43
10	0.2287	0.0614	0.0000	1.49	0.6217	14.35	16.29
11	0.1897	0.0605	0.0010	2.19	0.5212	12.09	16.26
12	0.2994	0.0133	0.0949 [†]	0.24	0.3581	12.15	18.48
13	0.3000	0.0394	0.1093 [†]	0.63	0.5310	9.02	13.45
14	1.1745	0.0663	0.0575 [†]	1.40	0.2283	11.66	16.16
15	0.4809	0.0183	0.1071 [†]	0.57	0.4373	20.02	15.95
16	0.6910	0.0200	0.1050 [†]	0.11	1.0000	15.97	19.05
17	1.3082	0.1082	0.0827 [†]	0.00	0.2379	7.34	10.48
18	0.4330	0.0769	0.0236 [†]	1.56	0.5292	7.00	19.90
19	0.5943	0.1034	0.0694 [†]	2.11	0.4851	11.88	11.57
Mean ± s.d.	0.4555 ± 0.3779	0.0584 ± 0.0289	0.0492 ± 0.0447	1.29 ± 1.10	0.5100 ± 0.1989	15.84 ± 9.84	16.13 ± 3.57
Biliary atresia							
20	0.1370	0.0465	0.0000	4.58	0.3100	19.48	21.51
21	0.1405	0.0231	0.0527 [†]	0.99	0.2088	29.60	26.39
22	0.0483	0.0298	0.0333 [†]	4.23	0.4537	33.64	31.70
23	0.2216	0.0495	0.0028	1.44	0.2490	21.70	19.12
24	0.3199	0.0768	0.0095	1.74	0.3881	12.81	11.59
25	0.1075	0.0571	0.0143	2.41	0.3751	18.64	14.01
26	0.2073	0.0663	0.0000	21.7	0.5578	14.58	15.09
27	0.1279	0.0526	0.0000	2.84	0.3716	17.22	19.02
28	0.1589	0.0638	0.0000	4.10	0.6148	13.40	15.68
30	0.0939	0.0547	0.0000	4.57	0.7381	12.88	18.28
31	0.0806	0.1036	0.0000	3.51	0.3785	9.67	9.66
32	0.0526	0.1328	0.0005	6.35	0.4466	9.81	7.50
33	0.3065	0.0730	0.0000	0.58	0.6102	13.31	13.70
Mean ± s.d.	0.1540 ± 0.0876	0.0638 ± 0.0291	0.0087 ± 0.0016	4.54 ± 5.42	0.4386 ± 0.1540	17.44 ± 7.28	17.17 ± 6.67
Choledochal cyst							
34 (Before)	0.1005	0.0539	0.0010	7.24	0.7266	14.14	18.22
34 (After)	0.1419	0.0348	0.0000	0.64	1.0000	24.67	28.74
Alagielle's syndrome							
35	0.2455	0.0572	0.0144	3.90	0.3357	15.20	13.97

*All k_R values to be multiplied by 10^{-3} .

[†]Patients in whom the model incorporating intrahepatic bile duct compartment is preferred in terms of the AIC and SC.

this study is that an accurate mechanistic picture of hepatocyte function could be obtained in terms of the extraction (k_{21}), reverse-binding (k_{12}) and excretion (k_3) constants. Such quantification clearly circumvents problems associated with qualitative visual assessment and can be used to evaluate patient hepatic performance as a function of time. Another important

feature is that a theory consistent with current physiological knowledge of hepatocyte disease can be applied. Where it is suspected, for example, that intrahepatic bile ducts may be obliterated or nonfunctional a model can be applied whereby the validity of such assumptions are objectively and readily tested. This feature adds to the versatility of this technique and

TABLE 4
Liver Function Test Results for Pediatric Population

Liver function tests*	Neonatal hepatitis	Biliary atresia	Choledochal cyst	Alagielle's syndrome
Total protein (g · L ⁻¹)	62 ± 8	63 ± 6.9	62	66
Albumin (g · L ⁻¹)	40 ± 5	37 ± 4.5	25	45
Globulin (g · L ⁻¹)	21 ± 7	27 ± 2.7	37	21
Total bilirubin (μmole · L ⁻¹)	212 ± 103	242 ± 93	133	256
Direct bilirubin (μmole · L ⁻¹)	121 ± 64	134 ± 63	70	203
Indirect bilirubin (μmole · L ⁻¹)	91 ± 45	98 ± 41	63	53
Alkaline phosphatase (IU · L ⁻¹)	889 ± 722	1019 ± 735	308	886
Aspartate aminotransferase (IU · L ⁻¹)	213 ± 114	418 ± 205	40	673
Alanine aminotransferase (IU · L ⁻¹)	203 ± 198	191 ± 106	24	443
γ-glutamyl transpeptidase (IU · L ⁻¹)	176 ± 125	458 ± 570	131	75

*Values provided as mean ± s.d.

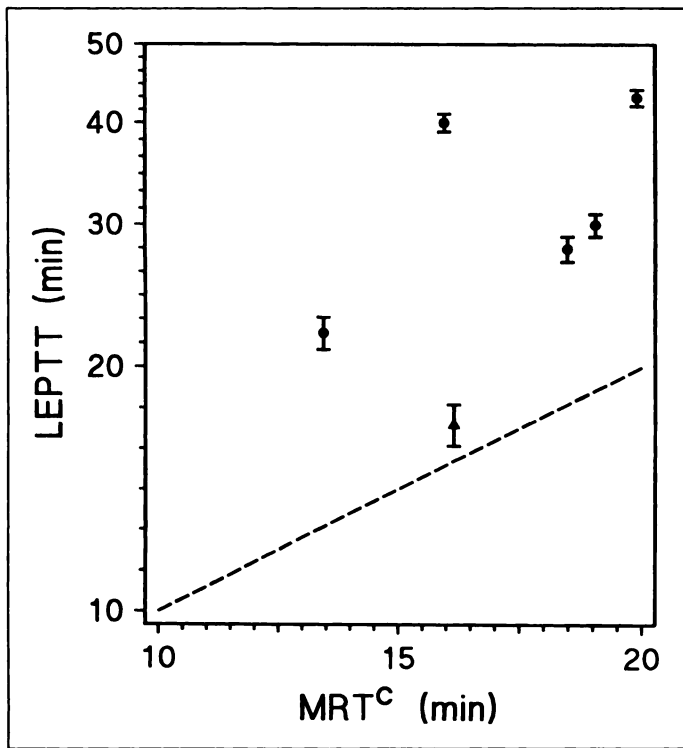


FIGURE 5. Representation of leading edge parenchymal transit times determined by measurement in relation to compartmental mean residence times in infants who demonstrated biliary drainage. Equivalence relationship (— —) is also depicted.

it can be anticipated that this treatment is easily extendable to other biliary and hepatocellular syndromes.

Other important results of this work concern the measurement of LEPTT and its relationship to hepatocyte mean residence times. This measurement, when performed correctly, can provide useful inference of bile duct patency from a functional perspective rather than a qualitative one. Such information is desirable in both the adults and infants as biliary tract disease is a known precursor to hepatocyte disease.

The suggestion that a hepatic extraction performance index, k_{21}/k_{12} , should be considered was made in anticipation of assessing individual patient performance over a period of time. This was motivated by our initial observation that the health of our patients is not only proportional to their extraction index (k_{21}) but also inversely proportional to their reverse-binding coefficient (k_{12}). In our patient in whom the choledochal cystectomy was performed, the k_{21}/k_{12} ratio improved by a factor of 3.45 postsurgery. Though exhaustive clinical correlation is necessary, it is postulated that such an index has potential in assessing the benefits in surgery.

Finally, this methodological approach, used in conjunction with information obtainable from standard biochemical data and performed as a function of time, might enhance clinical assessments of hepatic dysfunction and prognosis within the framework of our current treatment regimes.

ACKNOWLEDGMENT

We thank Arthur Edwards, systems administrator at the University of the Witwatersrand Computer Center, for the help obtained in porting the software used in this study to our current UNIX operating system.

REFERENCES

- Gerhold JP, Klingensmith WC, Kuni CC, et al. Diagnosis of biliary atresia with radionuclide hepatobiliary imaging. *Radiology* 1983;146:499-504.
- Majd M, Reba RC, Altman RP. Effect of phenobarbital on ^{99m}Tc-IDA scintigraphy on the evaluation of neonatal jaundice. *Semin Nucl Med* 1981;XI:194-204.
- Ikeda S, Sera Y, Akagi M. Serial ultrasonic examination to differentiate biliary atresia from neonatal hepatitis—special reference to changes in size of the gallbladder. *Eur J Pediatr* 1989;148:396-400.
- El Tumi MA, Clarke MB, Barret JJ, et al. Ten minute radiopharmaceutical test in biliary atresia. *Arch Dis Child* 1987;62:180-184.
- Tarolo GL, Picozzi R, Palagi B, et al. Comparative quantitative evaluation of hepatic clearance of diethyl-IDA and para-butyl-IDA in jaundiced and non-jaundiced patients. *Eur J Nucl Med* 1981;6:539-543.
- Jaw TS, Wu CC, Ho YH, et al. Diagnosis of obstructive jaundice in infants: Tc-99m DISIDA in duodenal juice. *J Nucl Med* 1984;25:360-363.
- Love JE, Shaffer P, Fraser IA, et al. Pharmacokinetic studies of DISIDA disposition II clinical studies. *Eur J Nucl Med* 1988;14:436-440.
- Fraser IA, Shaffer P, Staubus AE, et al. DISIDA kinetics to measure liver function in dogs. *Nucl Med Commun* 1989;10:435-447.
- Krishnamurthy S, Krishnamurthy GT. Nuclear hepatology: where is it heading now? *J Nucl Med* 1988;29:1144-1148.
- Brown PH, Juni EJ, Lieberman DA, et al. Hepatocyte versus biliary disease: a distinction by deconvolutional analysis of technetium-99m-IDA time-activity curves. *J Nucl Med* 1988;29:623.
- Williams DL. Improvement in quantitative data analysis by numerical deconvolution techniques. *J Nucl Med* 1979;20:568-570.
- Doo E, Krishnamurthy GT, Eklem MJ, et al. Quantification of hepatobiliary function as an integral part of imaging with technetium-99m-mebrofenin in health and disease. *J Nucl Med* 1991;32:48-56.
- Juni JE, Keyes JW, Carter W, et al. Differentiation of obstructive from nonobstructive jaundice by deconvolutional analysis of hepatobiliary scans [Abstract]. *J Nucl Med* 1983;24(suppl):30.
- Howman-Giles R, Moase A, Gaskin K, Uren R. Hepatobiliary scintigraphy in pediatric population: determination of hepatic extraction fraction by deconvolutional analysis. *J Nucl Med* 1993;34:214-221.
- Lantsberg S, Boivin CM, Auld DA, et al. Assessment of quantitative methods of measuring hepatic function using Tc-99m iminodiacetic acid (IDA) scintigraphy. Abstracts of the 18th annual meeting of the British Nuclear Medicine Society. *Nucl Med Commun* 1990;11:203.
- Lantsberg S, Lanchbury EE, Drolz ZA. Evaluation of bile duct complications after orthotopic liver transplantation by hepatobiliary scanning. *Nucl Med Commun* 1990; 11:761-769.
- Hawkins RA, Gambhir SS, Huang SC, et al. Tracer kinetic modeling approaches to HIDA studies: application to liver transplant patients. *J Nucl Med* 1987;28:653.
- Hawkins RA, Hall T, Gambhir SS, et al. Radionuclide evaluation of liver transplants. *Semin Nucl Med* 1988;XVIII:199-212.
- Gambhir SS, Hawkins RA, Huang SC, et al. Tracer kinetic modeling approaches for the quantification of hepatic function of technetium-99m DISIDA and scintigraphy. *J Nucl Med* 1989;30:1507-1518.
- Landaw EM, DiStefano JJ. Multiexponential, multi-compartmental and noncompartmental modeling. II. Data analysis and statistical considerations. *Am J Physiol* 1984;246:R665-677.
- Chen C-T. *Introduction to linear system theory*. New York, NY: Holt, Rinehart and Winston, 1970.
- Butkov E. Concepts of the theory of distributions. In: Hamermesh M, ed. *Mathematical Physics*. Menlo Park, CA: Addison-Wesley; 1968:221-257.
- Klingensmith WC. Hepatobiliary imaging: normal appearance and normal variations. In: Gottschalk A, Hoffer PB, Potchen, eds. *Diagnostic nuclear medicine*, 2nd ed. Baltimore, MD: Williams and Wilkins; 1988;2:575-581.
- Vera DR, Stadalnik RC, Trudeau WL, et al. Measurement of receptor concentration and forward-binding rate constant via radio-pharmacokinetic modeling of technetium-99m-galactosyl-neoglycoalbumin. *J Nucl Med* 1991;32:1169-1176.